RSC Advances

PAPER

View Article Online
View Journal | View Issue

Cite this: *RSC Adv.*, 2020, **10**, 20138

Influence of liquid bridge formation process on its stability in nonparallel plates†

Xiongheng Bian, Haibo Huang‡* and Liguo Chen‡*

The formation of a liquid bridge in non-parallel plates is very common and the stability (whether or not it can move spontaneously) of such liquid bridges has been studied a lot for industry, *e.g.* in printing applications. It is generally considered that the liquid bridge stability is determined by Contact Angle (CA), Contact Angle Hysteresis (CAH), the position of the liquid bridge (represented as P) and the dihedral angle (θ) between non-parallel plates. The stability equation is $\theta = f(\mathrm{CA}, \mathrm{CAH}, P)$. Since P is a process quantity, which is difficult to determine, so it is also difficult to obtain the critical equation for the stability of the liquid bridge. In the previous study (*J. Colloid Interface Sci.*, 2017, **492**, 207–217), based on the fitting simulation results, the critical equation about CA, CAH and θ is obtained, as $\theta = f(\mathrm{CA}, \mathrm{CAH})$. However, in some special cases, the results are still biased (*e.g.* the weak hydrophilic situation). In this paper, unlike simulation, we get the critical equation $\theta = f(\mathrm{CA}, \mathrm{CAH})$ from a theoretical point of view. For the first time, by in-depth analysis of the process of liquid bridge formation, the theoretical calculation equation of P is obtained as $P = f(\mathrm{CA}, \mathrm{CAH}, \theta)$. And then, combining the equations $\theta = f(\mathrm{CA}, \mathrm{CAH}, P)$ and $P = f(\mathrm{CA}, \mathrm{CAH}, \theta)$, the theoretical equation is obtained. A lot of simulations and experiments were performed to verify our theoretical equation. Furthermore, comparing our equation with the previous equation, it was found that our equation is more consistent with the experimental results (error less than 0.2°). Finally, the importance of considering the liquid bridging process (the function of P) for stability analysis is illustrated by comparing the results with those not considered (the difference is more than 20% in some cases). The outputs of this paper provide in-depth theoretical support for the analysis and application of liquid bridges.

Received 17th April 2020
Accepted 20th May 2020

DOI: 10.1039/d0ra03438j

rsc.li/rsc-advances

1. Introduction

The formation of a liquid bridge is a common phenomenon of droplets, and is widespread in various industrial applications.[1–5] As a common type, the liquid bridge in non-parallel plates has been widely used in droplet collection,[6] oil–water separation[7] and other microfluidics applications[8–10] due to its directional spontaneous motion. In the last few decades, the stability of this kind of liquid bridge (whether it can move spontaneously) has been discussed a lot.[11–13] The different Contact Angles (CAs) generated by the hydrophilic non-parallel plate structure lead to the different Laplace pressure on the opposite side of the liquid bridge, which propels the liquid bridge to move. Meanwhile, the Contact Angle Hysteresis (CAH) provides the hysteresis for the change of CAs, which prevents the motion of the liquid bridge, so as to maintain the stability of the liquid bridge.[14] Therefore, it is generally believed that the stability of the bridge is mainly determined by the properties of the surface (CA and CAH), the structure of nonparallel plates (the dihedral angle θ). In addition, Ataei *et al.*[15] proposed that the stability of the liquid bridge was also affected by the bridge position. Therefore, the critical equation should be $\theta = f(\mathrm{CA}, \mathrm{CAH}, P)$. Since P is a process quantity, which is mainly determined by the bridge formation process and difficult to determine. Then, it is also difficult to obtain the critical equation for the stability of the liquid bridge. In the previous study, Luo *et al.*[14] analyzed the equation $\theta = f(\mathrm{CA}, \mathrm{CAH}, P)$ and gave a rough estimate of the stability of the liquid bridge by ignoring the influence of the parameter P. By fitting the experimental and simulation results, Ataei *et al.* obtained the critical equation as $\theta = f(\mathrm{CA}, \mathrm{CAH})$ instead of $\theta = f(\mathrm{CA}, \mathrm{CAH}, P)$, to judge the stability of the liquid bridge in the hydrophilic nonparallel plates. The existing methods all choose to avoid the calculation of P.

However, there are still three shortcomings in the current research. Firstly, since the critical equation $\theta = f(\mathrm{CA}, \mathrm{CAH})$[16] is obtained by fitting the experimental and simulation results, and the influence of P is ignored, the equation works well in most cases, but there are still deviations in some special cases (for

Robotics & Microsystem Center, Collaborative Innovation Center of Suzhou Nano Science and Technology, Soochow University, Suzhou 215123, China. E-mail: hbhuang@suda.edu.cn; chenliguo@suda.edu.cn

† Electronic supplementary information (ESI) available. See DOI: 10.1039/d0ra03438j

‡ Present addresses: Robotics & Microsystem Center & Collaborative Innovation Center of Suzhou Nano Science and Technology, Soochow University Suzhou 215123, China.

example, the weak hydrophilic situation). Secondly, since P is decided by the liquid bridge formation process, then, how to calculate the value of P by analyzing the process of liquid bridge formation is still unknown. Third, the importance of considering the process of liquid bridge formation is still unknown.

In this paper, based on equation $\theta = f(\text{CA, CAH, } P)$, we try to find a theoretical method to calculate P, so as to obtain a theoretical equation about $\theta = f(\text{CA, CAH})$. First, from a geometric perspective, the critical equation about $\theta = f(\text{CA, CAH, } P)$ was given out. Then, through theoretical analysis, the influence of bridge formation process on its post-bridge position is studied, and the theoretical calculation equation $P = f(\text{CA, CAH, } \theta)$ is obtained, and verified by simulations. Furthermore, the theoretical curves, as $\theta = f(\text{CA, CAH})$, for judging the stability of the liquid bridge are obtained for the first time. After that, the theoretical curves are compared with the existing fitting equation,[16] and found it more consistent with the experimental results in the weak hydrophilic situation. Finally, the situation where the formation process needs to be considered are identified. The outputs of this paper provide a new theoretical support for the analysis and application of the liquid bridge.

2. Theoretical analysis of liquid bridge in nonparallel plates

According to the geometric structure of Fig. 1, the equations about CAs can be obtained (the CA near the cusp α_1 and the CA away from the cusp α_2):

$$\frac{\pi+\theta}{2} + \arcsin\left[\frac{S\sin(\theta/2)}{R_1}\right] = \alpha_1 \quad (1)$$

$$\frac{\pi-\theta}{2} + \arcsin\left[\frac{(S+L_D)\sin(\theta/2)}{R_2}\right] = \alpha_2 \quad (2)$$

Here, O is the cusp of the nonparallel plates, θ is the angle between the nonparallel plates, L_D is the length of the droplet, and S is the minimum distance between the droplet and cusp. R_1 and R_2 are the radius of curvature on the left and the right side of the droplet respectively. Then, combined with previous researches,[14,16–18] the stability of the liquid bridge are discussed:

• For the case of inward motion: eqn (1) and (2) can be transformed into the equations about R, as $R_1 = -\dfrac{S\sin\dfrac{\theta}{2}}{\cos\left(\alpha_1 - \dfrac{\theta}{2}\right)}$ and $R_2 = -\dfrac{(S+L_D)\sin\dfrac{\theta}{2}}{\cos\left(\alpha_2 + \dfrac{\theta}{2}\right)}$. According to Laplace equation, $|R_1| < |R_2|$ is necessary to make the spontaneous inward motion. Besides that, CAs also have to satisfy $\alpha_1 = \alpha_a$ and $\alpha_2 = \alpha_r$ (subscripts a and r represent the advancing and receding angles of the droplets on the surface, respectively). Therefore, it can be found that when $\alpha_a < \dfrac{\pi}{2} + \dfrac{\theta}{2}$ and $\theta > \alpha_{CAH}$, the requirements can be met. More precisely, the conditions of inward motion can be written as:

$$\theta > 2\arctan\left[\frac{S\cos\alpha_r - (S+L_D)\cos\alpha_a}{(S+L_D)\sin\alpha_a + S\sin\alpha_r}\right] \quad (3)$$

and $\alpha_a < \dfrac{\pi}{2} + \dfrac{\theta}{2}$ (the details are offered in the ESI 1†). From eqn (3), it can be inferred that the stability conditions of the liquid bridge on the hydrophilic surface are mainly determined by α_a, α_{CAH} and L_D/S. Here, L_D/S is used to represent the position of liquid bridge (value of P).

• For the case of outward motion: to achieve the spontaneous outward motion, CAs have to satisfy $\alpha_1 = \alpha_r$ and $\alpha_2 = \alpha_a$. Therefore, the conditions of θ is:

$$\theta < 2\arctan\left[\frac{S\cos\alpha_a - (S+L_D)\cos\alpha_r}{(S+L_D)\sin\alpha_r + S\sin\alpha_a}\right] \quad (4)$$

and the equation $\alpha_a > \dfrac{\pi}{2} + \dfrac{\theta}{2}$ needs to be satisfied. From these inequations, it can be found that:

(1) Only on the hydrophobic surface can the liquid bridge move outwards spontaneously.

(2) θ will be smaller and approaching to zero with the decreasing of L_D/S. However, with the spontaneous outward motion, L_D/S has to be smaller, so the liquid bridge cannot exit nonparallel plates completely.

In conclusion, the critical condition for the liquid bridge to move inward is $\theta > 2\arctan\left[\dfrac{S\cos\alpha_r - (S+L_D)\cos\alpha_a}{(S+L_D)\sin\alpha_a + S\sin\alpha_r}\right]$, and the critical condition for the liquid bridge to move outward is $\theta < 2\arctan\left[\dfrac{S\cos\alpha_a - (S+L_D)\cos\alpha_r}{(S+L_D)\sin\alpha_r + S\sin\alpha_a}\right]$. It shows that the conditions for stable liquid bridges should be associated with the coupling of CA, CAH, θ and L_D/S. Among them, CA, CAH and θ are determined by the surface properties and structural properties of nonparallel plates. L_D/S is determined by the formation process of the liquid bridge. Then, in next sections, the influence of liquid bridge formation on L_D/S is discussed.

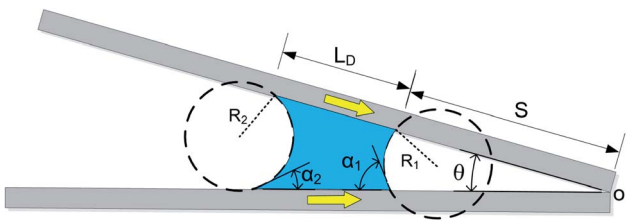

Fig. 1 The model of the droplet pinned in hydrophilic nonparallel plates.

3. The improved simulation process of liquid bridge formation

In order to study the influence of liquid bridge formation on L_D/S, the formation process of liquid bridge was simulated through surface evolver. A friction model based on Santos and White[19] was used to implement CAH. By this method, the contact lines will only move if the CA is greater than the advancing angle or less than the receding angle. Different from previous simulation

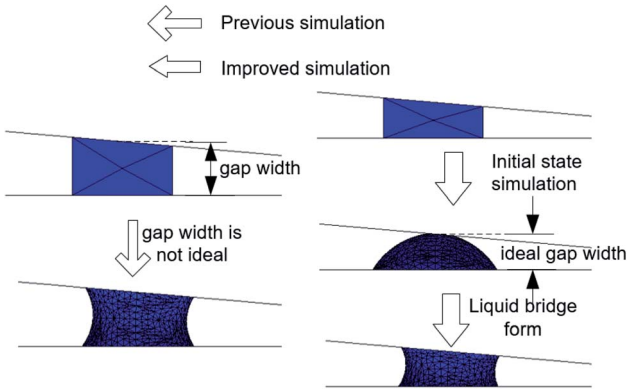

Fig. 2 Compare the improved and previous simulation processes.

method,[16] as shown in Fig. 2, the simulation process was improved to make it more in line with the actual liquid bridge forming process. The improved simulation is composed of two steps: initial state simulation and liquid bridge formation simulation. The first step is the initial state simulation, which aims to simulate the instantaneous state of the droplet when it just touches the upper plate. In this process, the wetting angle of the upper plate is set to 70° and the wetting angle of the upper plate is set to nearly 180° to ensure that droplets will not adhere to the upper plate. In addition, the initial droplet is ensured to be spherical by setting CAH = 0. By doing this, the gap width is similar to the ideal width (where the droplet just touches the upper plate). The second step is the liquid bridge formation simulation, which was carried out by resetting the CA of the upper plate to the same as the bottom plate (70°).

4. The influence of bridge forming process on L_D/S

In order to better understand the influence of bridge forming process on L_D/S, the formation process is theoretically discussed and verified by simulations and experiments.

4.1 Analysis of the influence of the formation of liquid bridge on L_D/S

As shown in Fig. 3b, geometrically, the initial value of the L_D/S can be written as eqn (5) (the calculation process is offered in the ESI 2†).

$$\frac{L_{DI}}{S_I} = \frac{2\sin\alpha_a\tan\theta}{\cos\theta - \cos\alpha_a + \sin\theta\tan\theta - \sin\alpha_a\tan\theta} \quad (5)$$

During the bridge forming process, with the droplet wetting along the up-plate and receding on the bottom plate, as shown in Fig. 3b and c, L_{DI} goes down to L_{DBT}, and S_I goes up to S_{BT} (here, subscripts I, BT and UP represent the initial state, bottom plate and upper plate respectively). Since the exist of CAH, L_{DBT} is larger than L_{DUP} and S_{BT} is smaller than S_{UP}, but these difference are very small and negligible when calculating the value of L_D/S (the details is demonstrated in Section 4.1.2).

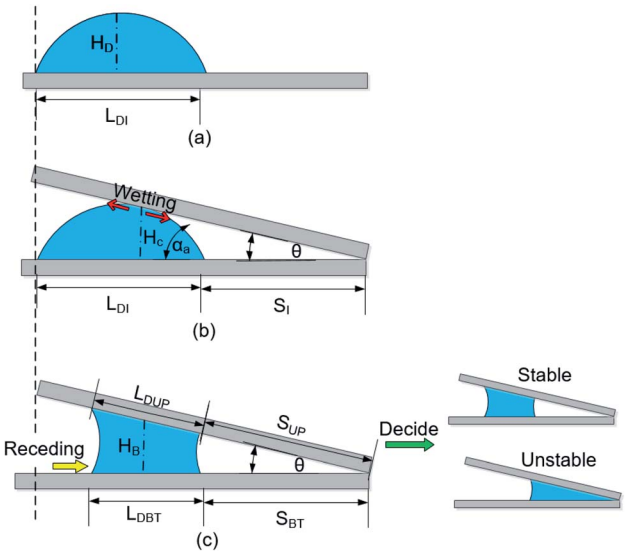

Fig. 3 The model of liquid bridge forming process (a) before bridge forming process (b) at the beginning of bridge forming process (c) after bridge forming process (which decide the later stability).

Therefore, it can be found that $\frac{L_{DI}}{S_I} > \frac{L_{DBT}}{S_{BT}} \approx \frac{L_{DUP}}{S_{UP}}$. L_D/S after bridge forming can be calculated by:

$$\frac{L_D}{S} = \frac{2\sin\alpha_a\tan\theta}{\cos\theta - \cos\alpha_a + \sin\theta\tan\theta - \sin\alpha_a\tan\theta} - \Delta\frac{L_D}{S} \quad (6)$$

Here, $\Delta\frac{L_D}{S} = \frac{L_{DI}}{S_I} - \frac{L_{DUP}}{S_{UP}}$, $\Delta\frac{L_D}{S}$ represents the change of $\frac{L_D}{S}$ induced by the bridge formation process and is mainly affected by the corner angle θ, CA and CAH. Then, how can $\Delta(L_D/S)$ be calculated in terms of θ, α_a, CAH is discussed.

4.1.1 The effect of the angle θ and advancing angle α_a to the value of $\Delta(L_D/S)$. Without considering the effect of CAH, the formation process of the liquid bridge in hydrophilic nonparallel plates is discussed and the calculation equation of $\Delta(L_D/S)$ is given below.

In fact, the process of liquid bridge formation is also the process that liquid droplets wetting along the upper plate. Since α_1 is always greater than α_2 when in the hydrophilic nonparallel plates (according to eqn (1) and (2)), the inner contact line stays still while the outer contact line recedes, that is, $S_I \approx S_{UP}$. In addition, in order to simplify the calculation, the liquid bridge can be seen as cylindrical in shape after its formation, and its average height is H_B (as shown in Fig. 3c). Such height is similar to the height of the contact point (marked as H_C, as shown in Fig. 3b) when the upper plate contacts the droplets and is also the height of the droplets in the initial state (marked as H_D, as shown in Fig. 3a). Then, the average height and volume after the formation of the liquid bridge can be written as:

$$H_B \approx (S_{UP} + L_{DUP}/2)\tan\theta \quad (7)$$

$$V \approx \pi H_B\left(\frac{L_{DUP}}{2}\right)^2 \quad (8)$$

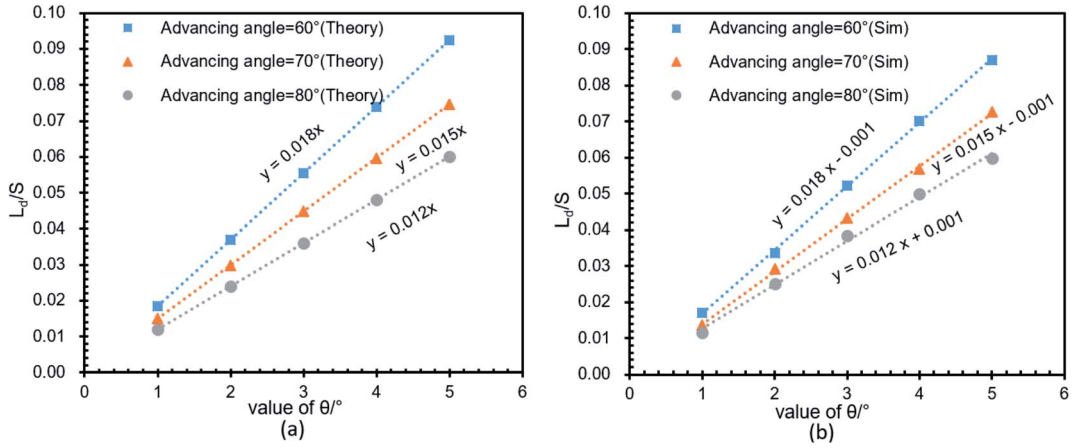

Fig. 4 Verify the relationship between $\Delta(L_D/S)$, θ and α_a in eqn (11). (a) The theoretical relationship between $\Delta(L_D/S)$ and θ with different α_a. (b) The simulation results between $\Delta(L_D/S)$ and θ with different α_a.

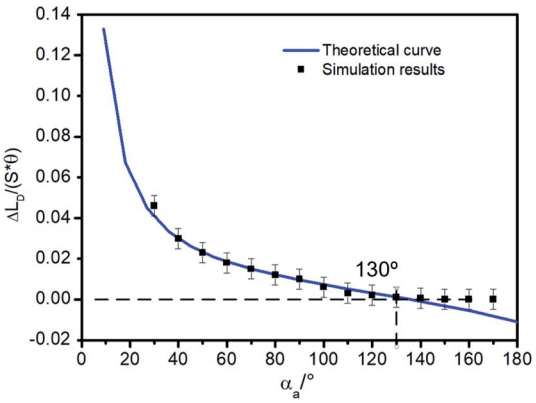

Fig. 5 The curve of $\Delta(L_D/S)$ with α_a based on numerical calculation and verified by simulations.

Meanwhile, for the initial droplet, the average height and volume before the formation of the liquid bridge can be written as (the calculation process is offered in the ESI 3†):

$$H_D = L_{DI}/(2\sin\alpha_a)(1-\cos\alpha_a) \quad (9)$$

$$V = \pi {H_D}^2\left(\frac{H_D}{1-\cos\alpha_a} - \frac{H_D}{3}\right) \quad (10)$$

According eqn (7)–(10), $H_B \approx H_D$ and $S_I \approx S_{UP}$, eliminate the variables (H_B, H_D, V) in them and substitute into the equation $\Delta\frac{L_D}{S} = \frac{L_{DI}}{S_I} - \frac{L_{DUP}}{S_{UP}}$, the expression of $\Delta\frac{L_D}{S}$ without considering CAH can be written as:

$$\Delta\frac{L_D}{S} = \frac{L_{DI}}{S_I} - \frac{L_{DUP}}{S_{UP}} \approx \left[\frac{2\sin\alpha_a}{1-\cos\alpha_a} - 2\sqrt{\frac{1}{1-\cos\alpha_a} - \frac{1}{3}}\right] \times \theta \quad (11)$$

To verify the relationship between $\Delta(L_D/S)$, θ and α_a in eqn (11), verification simulations by surface evolver are carried out. In these simulations, CAHs are ignored, α_a has different values (varying from 60° to 80°) and θ also has different values (varying

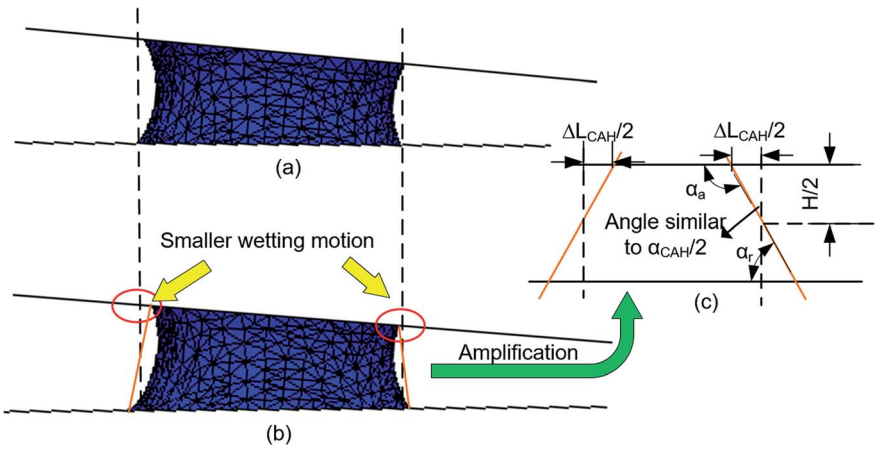

Fig. 6 Analysis about the CAH effect based on simulation (a) simulation result without CAH (b) simulation result with $\alpha_{CAH} = 30°$ (c) theoretical analysis model about the effect of α_{CAH}.

from 1° to 6°). According to the simulation results shown in Fig. 4b, the curves are approximately linear. The approximate lines with different α_a are $\Delta\frac{L_D}{S} = 0.018\theta - 0.001$, $\Delta\frac{L_D}{S} = 0.015\theta - 0.001$ and $\Delta\frac{L_D}{S} = 0.012\theta + 0.001$ respectively. Compared with the theoretical results obtained from eqn (11), as shown in Fig. 4a (the approximate lines are $\Delta\frac{L_D}{S} = 0.018\theta$, $\Delta\frac{L_D}{S} = 0.015\theta$ and $\Delta\frac{L_D}{S} = 0.012\theta$ respectively), the theoretical curves and the simulation curves are basically the same.

In addition, more simulations were carried out to verify the correctness of the eqn (11) for a larger range of α_a (varying from 30° to 170°). Simulation results are shown in Fig. 5. The solid line is the theoretical curve obtained by the eqn (11) and the points are the simulations results. The theory and simulation results are consistent. When α_a is greater than 130°, $\Delta(L_D/S)$ is approximately 0, so in this case, the bridge formation process does not need to be considered.

4.1.2 The effect of CAH to the value of $\Delta(L_D/S)$. $\Delta(L_D/S)$ is also affected by CAH. The simulation screenshots about liquid bridge after bridge forming process are shown in Fig. 6a (CAH = 0°) and Fig. 6b (CAH = 30°). It can be found that when the CAH is larger, the corresponding wetting motion is smaller (L_{DUP} decrease, L_{DBT} increase). Assuming the change in L_{DUP} caused by CAH is ΔL_{CAH} and the upper and bottom plates are parallel. Hence, as shown in Fig. 6c, the simplified analytical model about the effect of CAH can be obtained. The dashed line indicates the position of the liquid bridge when CAH is not considered, while the solid line indicates the position of the liquid bridge when CAH is considered. The difference between the two positions on upper plate is $\Delta L_{CAH}/2$. In addition, when the liquid bridge is stable, the angle between the bridge and the upper plate should be approximately equal to α_{CAH} (the CA on the upper plate is α_a and the CA on the bottom plate is α_r). So, the angle between the dashed line and the solid line is similar to

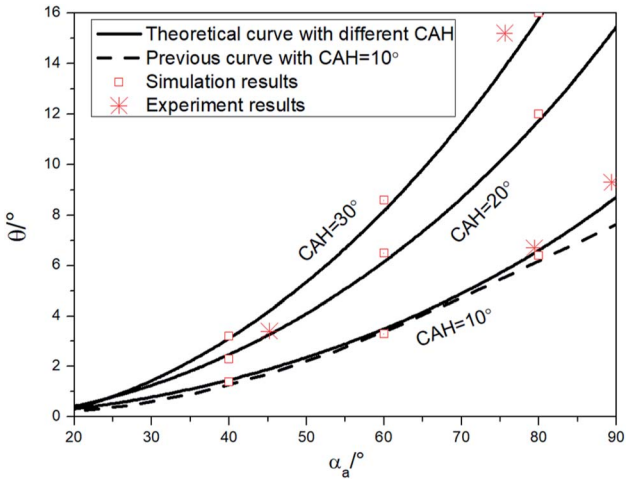

Fig. 8 Verify the theoretical curves with the simulations, experiment results and compare with previous study.

$\alpha_{CAH}/2$. From this relationship, the calculation equation of ΔL_{CAH} can be obtained:

$$\Delta L_{CAH} \approx H \tan(\alpha_{CAH}/2) \quad (12)$$

According to the structural equation ($H \approx S\theta$), it can be found $\Delta\frac{L_{CAH}}{S} \approx \tan\frac{\alpha_{CAH}}{2} \times \theta$. Combining the eqn (11), the equation of $\Delta(L_D/S)$ considering CAH can be obtained as:

$$\Delta\frac{L_D}{S} \approx \left(\frac{2\sin\alpha_a}{1-\cos\alpha_a} - 2\sqrt{\frac{1}{1-\cos\alpha_a} - \frac{1}{3}} + \tan\frac{\alpha_{CAH}}{2}\right) \times \theta \quad (13)$$

The relationship between $\Delta(L_D/S)$ and α_{CAH} is further analyzed by eqn (13) and simulations (obtained by surface evolver). The theoretical curves in Fig. 7 are obtained by eqn (13)

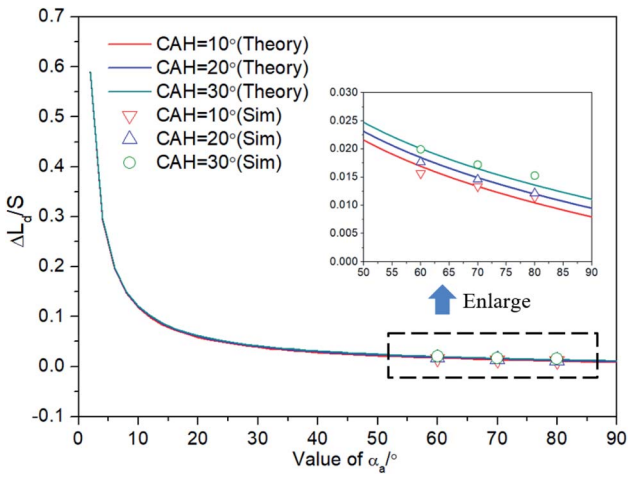

Fig. 7 Verify the relationship between $\Delta(L_D/S)$ and α_{CAH} in eqn (13) and demonstrate that the effect of α_{CAH} on $\Delta(L_D/S)$ is negligible.

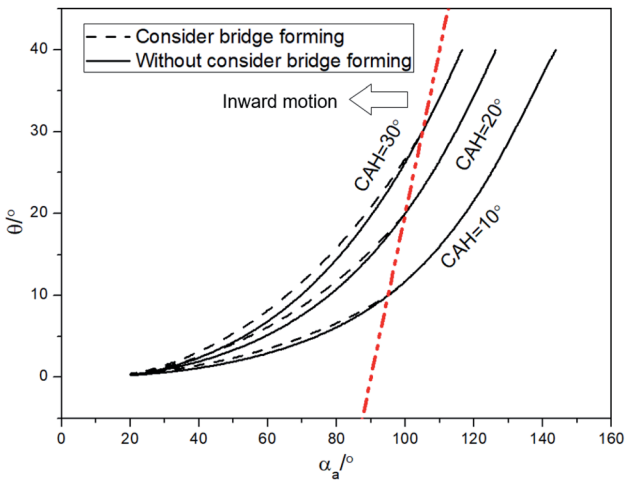

Fig. 9 Comparisons of results between considering and without considering bridge forming by theoretical analysis.

Table 1 Comparing about our method to other methods

Methods	Formation process	Range of stability	Significance
Equation analysis[14]	Without considered	Approximate range	Theoretical basis
Fitting by simulations[16]	Considered but not analyzed	Better when CA < 60°	First stability equation
Our method	Analyzed	Almost cases	Formation process analyzed

and the points in Fig. 7 are obtained through simulations. In these simulations, θ is set to 1° and α_{CAH} has three different values (varying from 10° to 30°). The following two points can be obtained:

(1) The curves almost coincide with each other at different α_{CAH}, indicating that the influence of α_{CAH} on $\Delta(L_D/S)$ is almost negligible.

(2) Considering the effect of α_{CAH}, as shown in the local enlarged image, the greater α_{CAH}, the greater $\Delta(L_D/S)$. The simulation results are also consistent with the prediction of eqn (13) (the maximum error is less than 0.002). The correctness of the equation is verified.

In conclusion, the influence of CAH on $\Delta(L_D/S)$ is so small and can be ignored, which explains why the theoretical model in the third section and eqn (6) and (7) can be used in this paper.

4.2 Verification about our critical equations by simulations and experiments

Substitute eqn (13) into eqn (6), and eqn (6) into eqn (4), and the theoretical curves for the stability determination of the liquid bridge in the hydrophilic nonparallel plates can be obtained (as shown in Fig. 8).

In order to verify these theoretical curves, simulations and experiments were carried out. Based on the simulation model of the third section, the simulation results are also obtained in the Fig. 8, which are found to be basically consistent with the theoretical curves (error less than 0.5°). In the experimental part, polystyrene (PS, $\alpha_a \approx 89.5°$, CAH ≈ 10.2°), poly(ethyl methacrylate) (PEMA, $\alpha_a \approx 79.4°$, CAH ≈ 10.5°), silicon ($\alpha_a \approx 44.5°$, CAH ≈ 21.2°) and glass ($\alpha_a \approx 75.6°$, CAH ≈ 29.2°) surfaces are adopted. The CAs and CAHs were measured using the sessile drop method and obtained by programming based on OpenCV. Measurements was repeated for five times for each surface. The experiments were carried out on the platform built in our previous study.[20] The bottom plate was placed horizontally, and then the downward movement of the upper plate was controlled by a micro motor. As soon as the upper plate came into contact with droplets at a low speed (0.01 mm s^{-1}), it stopped moving immediately. The critical angle of the stable liquid bridge was obtained by repeatedly locating θ when the liquid bridge was stable and unstable, and all the experiments were repeated five times and averaged for each case. The experimental results are shown in Fig. 8 (the asterisk marked), which also in line with the theoretical curves (the error was less than 0.5°). Comparing with the existing simulation fitting curve obtained by Alidad (the dotted line in Fig. 8),[16] the two have a good fit (the difference is less than 0.2°) in most situations, but slightly different when α_a is larger than 60°. It can be found that the critical angle of PS surface is about 9.2° by experiment (the asterisk marked), 8.8° by our theoretical curve (the solid line) and 7.5° by the previous study (the dotted line). It means that when α_a was greater than 60°, our curves are more consistent with the experimental results and has a better performance.

In conclusion, comparing our method with the previous methods, Table 1 can be obtained:

4.3 The situation where the process of liquid bridge formation needs to be considered

To illustrate the importance of considering the liquid bridging process, more research has been done. According to Fig. 5, when α_a is large than 130°, $\Delta(L_D/S)$ will goes down to zero, the change of $\Delta(L_D/S)$ can be neglected. But the importance of considering the process of liquid bridge formation in analyzing the stability of a liquid bridge when α_a is smaller than 130° is still unknow. Then, the situation of considering and without considering bridge forming was compared.

As shown in the Fig. 9, the theoretical curves (consider the process of liquid bridge formation) are obtained with different CAHs (the dotted line) by using the eqn (4), (6) and (13). Compared with the case that the formation process of liquid bridge is not considered (without consider the eqn (13)), it can be found that the difference between these two curves increases first and then decreases as α_a increases. If α_a is greater than 110°, the influence of the formation process of the liquid bridge on the stability can be ignored. But according to the research in Section 2, to achieve the inward motion, α_a also should smaller than $\frac{\pi}{2}+\frac{\theta}{2}$ (at the right part the red dotted line in Fig. 9). In this region, the results with and without considering the process of bridge formation are quite different (in some cases, the difference is more than 20%). Therefore, the process of bridge formation should be considered for inwards motion.

5. Summary and conclusion

In summary, experimental and numerical approaches as well as a theoretical analysis were employed to study the stability and formation process of a liquid bridge.

Compared with previous studies,[10,15,21–23] the paper provided the following new research progress.

(a) This research conclusion points out that the formation process of liquid bridge has influence on its later stability for the first time.

(b) The theoretical equation about the influence of formation process on bridge position is presented as $P = f(\mathrm{CA}, \mathrm{CAH}, \theta)$, and then, the theoretical curves for the stability determination of the liquid bridge are obtained as. The theoretical curves are verified by simulations and experiments.

(c) For inward motion, the process of bridge formation should be considered in all the cases.

Conflicts of interest

There are no conflicts to declare.

Acknowledgements

Authors acknowledge financial support from National Key R&D Program of China (2018YFB1304905), Natural Science Foundation of the Jiangsu Higher Education Institutions of China (17KJA460008) and Natural Science Foundation of Jiangsu Province of China (BK20171215).

References

1 S. Collignon, J. Friend and L. Yeo, Planar microfluidic drop splitting and merging, *Lab Chip*, 2015, **15**(8), 1942–1951.
2 L. Wang, M. Qiu, Q. Yang, Y. Li, G. Huang, M. Lin, T. J. Lu and F. Xu, Fabrication of Microscale Hydrogels with Tailored Microstructures based on Liquid Bridge Phenomenon, *ACS Appl. Mater. Interfaces*, 2015, 7(21), 11134–11140.
3 S. Kumar, Liquid Transfer in Printing Processes: Liquid Bridges with Moving Contact Lines, in *Annu Rev Fluid Mech*, ed. S. H. Davis and P. Moin, 2015, vol. 47, pp. 67–94.
4 H. Chen, T. Tang and A. Amirfazli, Liquid transfer mechanism between two surfaces and the role of contact angles, *Soft Matter*, 2014, **10**(15), 2503–2507.
5 D. J. Broesch and J. Frechette, From Concave to Convex: Capillary Bridges in Slit Pore Geometry, *Langmuir*, 2012, **28**(44), 15548–15554.
6 X. Heng and C. Luo, Bioinspired Plate-Based Fog Collectors, *ACS Appl. Mater. Interfaces*, 2014, **6**(18), 16257–16266.
7 C. Luo and X. Heng, Separation of oil from a water/oil mixed drop using two nonparallel plates, *Langmuir*, 2014, **30**(33), 10002–10010.
8 D. Baratian, A. Cavalli, D. van den Ende and F. Mugele, On the shape of a droplet in a wedge: new insight from electrowetting, *Soft Matter*, 2015, **11**(39), 7717–7721.
9 J. Hong, J. K. Park, B. Koo, K. H. Kang and Y. K. Suh, Drop transport between two non-parallel plates via AC electrowetting-driven oscillation, *Sens. Actuators, B*, 2013, **188**, 637–643.
10 Y. Huang, L. Hu, W. Chen, X. Fu, X. Ruan and H. Xie, Directional Transport of a Liquid Drop between Parallel-Nonparallel Combinative Plates, *Langmuir*, 2018, **34**(15), 4484–4493.
11 P. Concus and R. Finn, Discontinuous behavior of liquids between parallel and tilted plates, *Phys. Fluids*, 1998, **10**, 39–43.
12 T. Y. Chen, J. A. Tsamopoulos and R. J. Good, Capillary Bridges between Parallel and Nonparallel Surfaces and their Stability, *J. Colloid Interface Sci.*, 1992, **151**(1), 49–69.
13 W. Xu, Z. Lan, B. Peng, R. Wen, Y. Chen and X. Ma, Directional Movement of Droplets in Grooves: Suspended or Immersed?, *Sci. Rep.*, 2016, **6**, 18836.
14 C. Luo, X. Heng and M. Xiang, Behavior of a liquid drop between two nonparallel plates, *Langmuir*, 2014, **30**(28), 8373–8380.
15 M. Ataei, H. Chen and A. Amirfazli, Behavior of a Liquid Bridge between Nonparallel Hydrophobic Surfaces, *Langmuir*, 2017, **33**(51), 14674–14683.
16 M. Ataei, H. Chen, T. Tang and A. Amirfazli, Stability of a liquid bridge between nonparallel hydrophilic surfaces, *J. Colloid Interface Sci.*, 2017, **492**, 207–217.
17 J. W. Bush, F. Peaudecerf, M. Prakash and D. Quere, On a tweezer for droplets, *Adv. Colloid Interface Sci.*, 2010, **161**(1–2), 10–14.
18 L. Wang, H. Wu and F. Wang, Efficient transport of droplet sandwiched between saw-tooth plates, *J. Colloid Interface Sci.*, 2016, **462**, 280–287.
19 M. J. Santos and J. A. White, Theory and Simulation of Angular Hysteresis on Planar Surfaces, *Langmuir*, 2011, **27**(24), 14868–14875.
20 X. Bian, H. Huang and L. Chen, Motion of droplets into hydrophobic parallel plates, *RSC Adv.*, 2019, **9**(55), 32278–32287.
21 M. Ataei, T. Tang and A. Amirfazli, Motion of a liquid bridge between nonparallel surfaces, *J. Colloid Interface Sci.*, 2017, **492**, 218–228.
22 W. Wang and T. B. Jones, Moving droplets between closed and open microfluidic systems, *Lab Chip*, 2015, **15**(10), 2201–2212.
23 J. Berthier, *Microdrops and Digital Microfluidics*, 2008.

